

TERRESTRIAL LASER SCANNING – CIVIL ENGINEERING APPLICATIONS

A. Berenyi, T. Lovas, A. Barsi

Department of Photogrammetry and Geoinformatics, Budapest University of Technology and Economics
 aberenyi@mail.bme.hu

Commission V, WG V/3

KEY WORDS: Terrestrial laser scanning, accuracy analysis, laboratory tests, load test measurement, engineering survey

ABSTRACT:

Three dimensional terrestrial laser scanning has already proved its potential in several application fields, such as topography, archaeology, mining and cultural heritage protection. Beside these areas a new demand emerged: accurate point cloud acquisition and post-processed results in engineering survey. This technology could broaden the field of engineering survey, although the limited accuracy has to be carefully considered. In order to confirm the accuracy claimed by the manufacturer, the Department of Photogrammetry and Geoinformatics carried out two complex laboratory measurements, where not only the main accuracy values were examined but the effect of different materials, colours and the incident angle.

1. LABORATORY TESTS

1.1 Accuracy of distance measurement

The first laboratory test focused on the investigation of distance measurement accuracy. In theory, this can be described by simple mathematical equations, but particular circumstances and objects could have various influences on the result. The examination took place in the laboratory of the Department of Structural Engineering in 2006. A steel plate was bended to simulate different distances (with as small increment steps as 1 mm) from the instrument. Reference measurements were also done with a high precision digital calliper ensuring submillimeter accuracy (Figure 1).

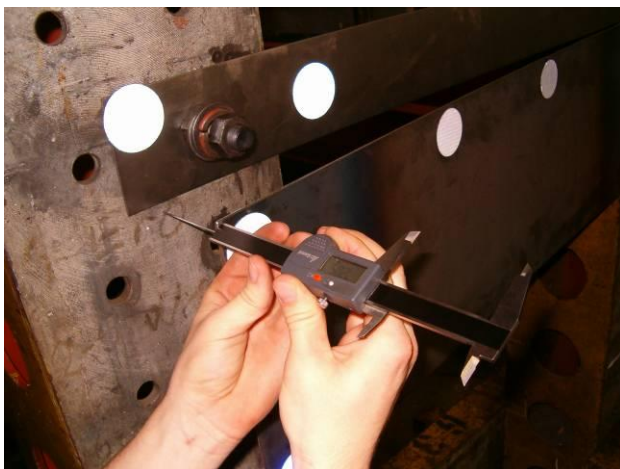


Figure 1: Reference measurement with high precision calliper

The plate was scanned with a Riegl LMS Z420i instrument in each position and reference points were measured as well. The results confirmed the factory given accuracy i.e. the RMSE remained under ± 5 mm.

1.2 Basic accuracy analysis: distance differences

During the second laboratory investigation 9 points were measured with a Riegl LMS Z420i and with a Leica TRCM 1203 total station in the laboratory of Department of Structural Engineering. The distances were calculated in every point combination (the result is a 9 by 9 matrix) based on the measurement results i.e. the coordinates from both instruments. Table 1 shows the differences between the calculated distance values in mm. Note that points labelled with SOCS (Scanner's Own Coordinate System) are measured with the scanner and the points labelled with numbers are the same points measured with the total station.

	SOCS								
	034	035	033	032	030	026	025	024	019
1	0	6,2	3,0	3,2	4,1	3,7	4,1	5,6	7,0
2	6,2	0	9,2	0,8	0,8	0,6	0,3	0,0	1,1
3	3,0	9,2	0	3,7	5,4	5,7	6,1	8,1	9,4
4	3,2	0,8	3,7	0	1,1	0,2	0,0	3,0	4,8
5	4,1	0,8	5,4	1,1	0	0,2	0,7	1,9	3,7
6	3,7	0,6	5,7	0,2	0,0	0	0,1	2,1	3,2
7	4,1	0,3	6,1	0,0	0,7	0,1	0	1,8	3,0
8	5,6	0,0	8,0	3,0	1,9	2,1	1,8	0	1,1
9	7,0	1,1	9,4	4,8	3,7	3,2	3,0	1,1	0

Table 1. Distance differences [mm]

Although detailed accuracy assessment needs error propagation calculations, these results may provide a good starting point. The authors like to emphasise that the evaluation mainly focuses on the procedure instead of the performance of the particular instrument. One of the main goals was to develop a method that is applicable for laser scanners regardless to manufacturer, brand or distance measurement method of the investigated scanner.

Note that the results highly depend on the used technology and other environment/geometry related factors.

1.3 Detailed accuracy analysis: 3D error propagation

Besides the already investigated distance measurement and distance difference analysis, the accuracy assessment of the 3D coordinates of every single point is also very important. Instead of analysing the coordinates provided by the instrument directly, the "raw" measurement results were processed, such as horizontal (H) and vertical (V) angle, and the previously qualified distance (D), in order to avoid rounding errors and to make the procedure instrument-independent:

$$(X, Y, Z) = f_{\text{TLS}}(H, V, D) \quad (1)$$

Note that the vertical angles were transformed from zenith distance to height angles in order to simplify the calculation of the error propagation.

$$\begin{aligned} X &= f_{\text{TLSX}}(H, V, D) = D \cdot \cos(H) \cdot \cos(V), \\ Y &= f_{\text{TLSY}}(H, V, D) = D \cdot \sin(H) \cdot \cos(V), \\ Z &= f_{\text{TLSZ}}(H, V, D) = D \cdot \sin(V). \end{aligned} \quad (2)$$

The squares of the standard deviation values of the coordinates (due to paper size limitations only the x value is shown) for every points (assuming that the measured values are independent):

$$\begin{aligned} \mu_x^2 &= g_x(H, V, D, \mu_V, \mu_H, \mu_D) = \left(\frac{\partial f_{\text{TLSX}}}{\partial H} \right)_0^2 \cdot \mu_H^2 + \\ &+ \left(\frac{\partial f_{\text{TLSX}}}{\partial V} \right)_0^2 \cdot \mu_V^2 + \left(\frac{\partial f_{\text{TLSX}}}{\partial D} \right)_0^2 \cdot \mu_D^2, \end{aligned} \quad (3)$$

a sample partial derivative:

$$\frac{\partial f_{\text{TLSX}}}{\partial H} = -D \cdot \sin(H) \cdot \cos(V). \quad (4)$$

Due to size limitations the further derivatives are not published. During the calculations the manufacturer's accuracy value (± 5 mm) was used as an initial value that was divided to three components (projections) parallel to the axes. The resultant of these projected vectors was calculated in order to verify the method:

$$\mu_i = \sqrt{\mu_{X_i}^2 + \mu_{Y_i}^2 + \mu_{Z_i}^2} = \pm 5 \text{ mm}. \quad (5)$$

The distance between two points:

$$\begin{aligned} d_{i,j} &= p_d(X_i, Y_i, Z_i, X_j, Y_j, Z_j) = \\ &= \sqrt{(X_i - X_j)^2 + (Y_i - Y_j)^2 + (Z_i - Z_j)^2}. \end{aligned} \quad (6)$$

The last step is the calculation of the error propagation function; with the squares of the standard deviation of the coordinates (assuming independent measurements):

$$\begin{aligned} \mu_{d_{i,j}}^2 &= \left(\frac{\partial p_d}{\partial X_i} \right)_0^2 \cdot \mu_{X_i}^2 + \left(\frac{\partial p_d}{\partial Y_i} \right)_0^2 \cdot \mu_{Y_i}^2 + \left(\frac{\partial p_d}{\partial Z_i} \right)_0^2 \cdot \mu_{Z_i}^2 + \\ &+ \left(\frac{\partial p_d}{\partial X_j} \right)_0^2 \cdot \mu_{X_j}^2 + \left(\frac{\partial p_d}{\partial Y_j} \right)_0^2 \cdot \mu_{Y_j}^2 + \left(\frac{\partial p_d}{\partial Z_j} \right)_0^2 \cdot \mu_{Z_j}^2. \end{aligned} \quad (7)$$

For example:

$$\frac{\partial p_d}{\partial X_i} = \frac{(X_i - X_j)}{d_{i,j}} \quad (8)$$

Table 2 shows the results of the calculation.

	SOCS								
	034	035	033	032	030	026	025	024	019
1		13,2	2,9	11,4	10,9	10,7	10,0	10,3	11,3
2	13,2		10,3	8,0	8,0	8,8	9,7	9,8	10,7
3	2,9	10,3		12,3	11,5	11,1	9,7	10,2	11,5
4	11,3	8,0	12,4		5,4	9,2	10,0	9,3	10,1
5	10,9	8,0	11,5	5,4		8,2	9,7	8,7	9,3
6	10,7	8,8	11,1	9,2	8,2		10,0	8,0	8,7
7	10,0	9,7	9,7	10,0	9,7	10,0		4,1	6,5
8	10,3	9,8	10,2	9,2	8,7	8,0	4,1		6,2
9	11,3	10,6	11,5	10,1	9,3	8,7	6,5	6,2	

Table 2. Deviation of the distances [mm]

For the better understanding, the main statistical values are gathered as follows:

$$\begin{aligned} \min(\mu_d) &= 2,9 \text{ mm}, \\ \text{avg}(\mu_d) &= 8,3 \text{ mm}, \\ \max(\mu_d) &= 13,2 \text{ mm}. \end{aligned} \quad (9)$$

The error propagation showed that the RMSE of the scanner's coordinate determination precision is the same that can be found in the technical specification; moreover, in most cases it is better.

1.4 Effect of materials and colours

After proving the accuracy claimed by the manufacturer, the emphasis was put on additional conditions that could affect the measurements and thus the quality of point clouds.

The second laboratory measurements were done in the laboratory of the Department of Structural Engineering in 2009. In the first test different materials often used at construction sites were investigated: natural wood bark, natural wood, sawn wood, varnished wood, steel, concrete, and brick. Each material was scanned from the same position. The post-processing of the separate point clouds was done by self developed software to minimize the effect of potential human error. The primary results were minimum, maximum and mean reflectivity values and average point density for each examined material. The results verified the expectations; the steel plate's reflectivity values were the smallest, because, as all shiny surfaces, it "diffuses" the laser beam. From the reflectivity point of view the brick is the best material, because its reflectivity is 1.7 times higher than that of the steel's (Table 3).

Material	N° of points	Reflectivity		
		Min.	Max.	Mean
brick	3597	0,227	0,281	0,251
concrete	3598	0,172	0,227	0,198
concrete (painted)	3626	0,141	0,227	0,186
natural wood	3597	0,168	0,250	0,204
natural wood bark	3590	0,184	0,254	0,216
raw wood	3597	0,203	0,231	0,232
sawn wood	3596	0,199	0,254	0,226
steel	3621	0,133	0,195	0,147
varnished wood	3652	0,203	0,270	0,246

Table 3: Reflectivity values of different materials

The effect of different colours on the reflected laser beam could be very important on construction sites, where the measurements have to be done prior to the final painting or surface treatment. A test object was painted in matte black, grey, and white colours (Figure 2), and the point cloud was analysed.

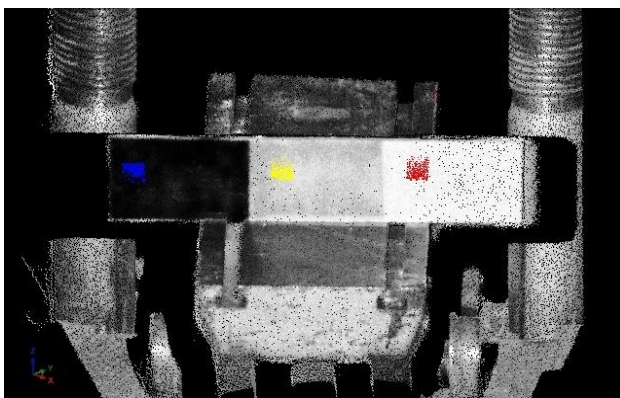


Figure 2: Test object with black, grey and white colour and its intensity representation (the coloured areas were investigated)

The results showed that the lowest reflectivity colour is black and the highest is white (Table 4). Note the significant difference between the two mean values!

Colour	N° of points (per dm ²)	Reflectivity		
		Min.	Max.	Mean
white	3640	0,207	0,258	0,232
grey	3640	0,156	0,211	0,181
black	3619	0,035	0,129	0,085

Table 4: Reflectivity values of different materials

1.5 Incident angle

Incident angle investigation could be very useful if measurements have to be accomplished e.g. in tiny rooms or narrow hallways, since the gathered data could contain errors (so called ghost points) because of the too small incident angle of the reflected laser beam. To avoid this type of measurement error, a threshold value of incident angle was derived.

In order to analyze the critical laser beam incident angle's effects on reflectivity, a steel object with two reflectors on its plane side was captured in different positions (Figure 3). The plate was scanned in 9 different positions, then the point density (per dm²), intensity, the coordinates of the marked points, and the angle of the plate in every single position were analyzed (Table 5).

Scan N°	Angle	N° of points (per dm ²)
1	90,00	2979
2	121,94	2662
3	137,52	2225
4	142,50	2070
5	158,49	1356
6	162,21	1113
7	168,33	798
8	176,73	353
9	179,14	127

Table 5: Incident angle and point density values

The results showed that the 8th scan of the steel plate provided significantly less points than the previous ones therefore this scan has been omitted from the evaluation process.

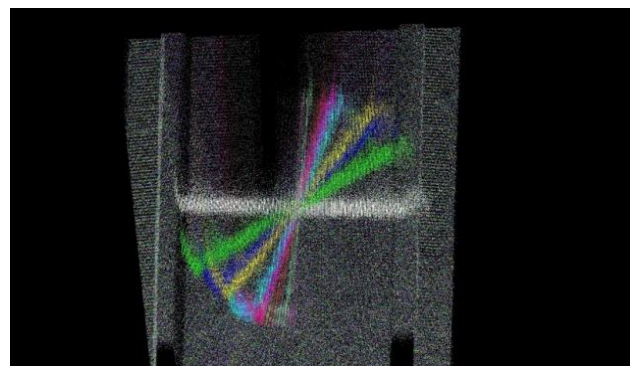


Figure 3: Test object for incident angle analysis and point clouds captured in different rotation angles

The parameters derived from the 7th scan showed that this scan contains outliers (gross errors); thus this scan has neither been taken into consideration. The evaluation provides reliable results above $\sim 10^\circ$ (170°). The authors would like to notice that this value strongly depends on the material of the scanned object, so this particular investigation provided reasonable results only for shiny steel surfaces.

2. APPLICATION EXAMPLES

2.1 Load test measurements

To confirm that terrestrial laser scanning is a reasonable data acquisition technique not only in the usual application fields but even in civil engineering applications. In the following a specific field of engineering survey, the load test of bridges will be discussed. This type of survey requires a lot of manpower, several instruments and a rather complex post-processing phase. Last, but not least, engineering survey needs to provide very accurate results (~ 1 mm). Although terrestrial laser scanning's accuracy is limited (± 5 mm), the application potential of this technique was proved during the measurement campaigns.

Load tests are usually following a very similar scenario, one particular test is described as follows. In the 0th load case the bridge is unloaded; reference measurements can be done. In the first load case (and any other cases except the intermediate unloaded cases) the bridge is loaded with 43 ton trucks according to the predefined load plan (different number of trucks located in different positions on the bridge). In each case the stresses and the displacements (vertical, horizontal, 3D) are measured with different types of instruments: strain gauges, high-precision levels, total stations. These measurement techniques have one feature in common: they could only provide data about discrete points. After all phases were measured, post-processing begins, and the expected (simulated and modelled) and calculated values are to be compared in order to validate the bridge's load capacity.

Megyeri Bridge

The load test of the cable-stayed Megyeri Bridge was done in August 2008. This bridge has a special structure that consists of nine bridge structures; additionally, this is the longest river bridge in Hungary (1 861 m). The scanned part is 591 m long and connects the left river bank (Pest side) with the Szentendrei Island (Figure 4).

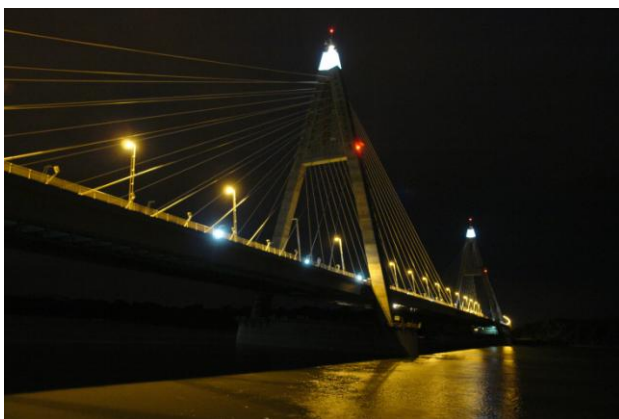


Figure 4: The Megyeri Bridge

By this particular load test two scanners were deployed to maximize the point density and to make sure that post-processing will provide the best results. Applying two scanners simultaneously was also necessary because the scanning positions were relatively close to the structure, and the data loss caused by too small incident angles is to be avoided.

The scanning resolution was set according to the time required by the high-precision levelling ($0,03^\circ$ for each scanner). One scan of a single load case resulted about 6 million (!) points, and lasted about 20 minutes.

The result data sets consists of single 3D points from which geometric elements have to be obtained during the post-processing phase; displacement of any point of the structure can be measured, no predefined points are needed. Note that identification of the point pairs could be difficult, thus geometric elements fitted on the evaluated part of the structure were used instead.

During the post-processing it was clearly seen that the bridge also moved during the more than 20 minute long load cases, so the laser scanner did not capture a snapshot, but the point cloud also "contains" the (minor) displacements occurred during the load case. The result of this effect can be clearly seen on Figure 5, the displacement values are more correlated on the side where the scanning has begun. Note that shaded areas could cause faulty post-processing results, thus these parts of the point cloud have to be removed prior to the post-processing.

The vertical displacement of the deck were calculated and compared to the results from high precision levelling as reference measurement. The results proved that terrestrial laser scanning could be used in such engineering survey applications. However, this state-of-the-art technology is not to be considered as a replacement of the existing technologies but as a useful additional data acquisition method.

A number of results were obtained that were not or cannot be measured during the load test, such as pylon tilt and cable movements. These results assured the authors to continue the examination of the 3D terrestrial laser scanning in other engineering applications.

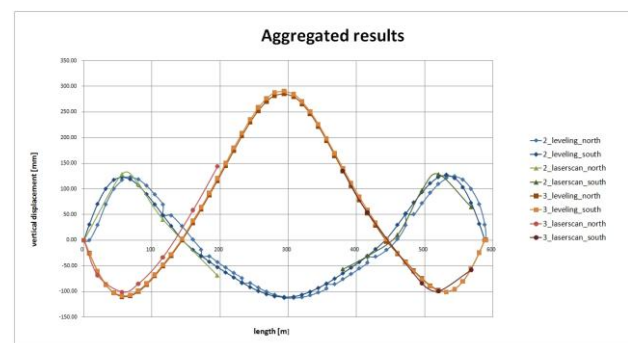


Figure 5: Aggregated results (high precision levelling and laser scanning) of the deck's vertical movement

Szebényi Motorway Bridge

Scanning the load test measurement of the motorway bridge at Szebény led to specific experiments; besides providing the usual deliverables (i.e. vertical displacements compared to and validated by high precision levelling), new scanning method was tested.

The applied Leica C10 laser scanner allowed the measurement even at extremely low temperature ($-4-5$ °C degrees). Since this bridge spans over a valley (not over a river), deploying the

scanner right under the girder was feasible, therefore displacements occurred in (or close to) the laser beam's direction were captured (Figure 6).

This kind of surveying from underneath the structure enables the analysis of the cross-sections, i.e. deriving the degree of asymmetry in displacements by capturing both sides of the structure. This scanning station allowed clear visibility to the pillar heads, therefore enabled the analysis of their horizontal movements (i.e. tilt distances and angles).



Figure 6: Scanning station underneath the Szebényi Bridge

2.2 Effect of ambient temperature for steel bridges - Erzsébet Bridge

Based on the positive experiences of several load tests, the technology's capability in other engineering applications was evaluated as well. One of these experiments is the investigation of the effect of ambient temperature on steel bridges.

Erzsébet bridge's span is 290 m, it connects Pest and Buda; its pylons are not standing in the Danube but on the riverbank.

To investigate the effect of the ambient temperature a scanning on 16th of November 2008 was made, as reference (0th) measurement. Two scanning positions were deployed, one on the left side of the Danube (Pest) and one on the right side (Buda). The ambient temperature was 7 °C, the traffic on the bridge was relatively low because it was scanned around midnight. This is very important because there are several public transportation bus lines cross the bridge that has major effect on bridge movements.

The scanning positions was deployed a bit farther from the bridge, thus the small incident angles could not cause problems or errors in the point cloud. Control points (6-7 tie points) were marked on each side of the Danube, to be able to make measurements for the second time in the same reference system. The second measurement was done in 26th of August 2009, in 22 °C ambient temperature (Figure 7).



Figure 7: Erzsébet bridge

The evaluation process included the vertical displacement investigation of the main cable and the deck. A 3D curve was fitted on the main cable in the 0th measurement's point cloud, and used as reference. Then the curve fitting was repeated in the second point cloud, and the differences were analyzed between the curves. The results showed that the maximal difference (i.e. the vertical displacement of the main cable) is 12.8 cm, and can be observed in the middle of the bridge (Figure 8).

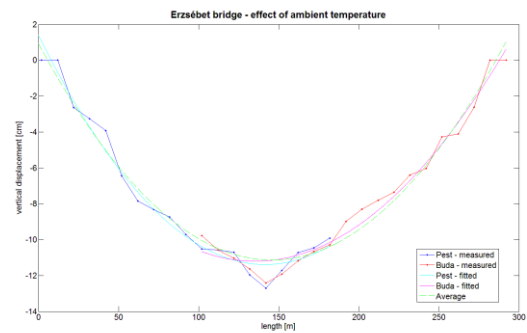


Figure 8: Erzsébet Bridge – evaluated results

The time frame of scanning was chosen around midnight again, to minimize the dynamic effect caused by the traffic.

The movement of the deck was calculated indirectly, because from the scanning positions only the lower structures of the bridge were visible, however these parts move together with the deck.

3. CONCLUSION

The state-of-the-art three dimensional terrestrial laser scanning has already proved its potential in several application fields, such as active quality control, monument protection, and mining applications.

The author's goal was to broaden the technology's application field in engineering survey applications as well. To confirm the factory given accuracy values laboratory tests were carried out, which proved the manufacturer's claim of accuracy. These tests focused not only on the 3D accuracy but on the effect of different materials, colours and incident angle.

Besides the laboratory investigation, the technology was tested in on-field applications as well. This new data acquisition technique is well applicable in engineering survey applications such as bridge load test measurements and detection of displacements caused by different ambient temperatures.

As every single geodetic measurement method, terrestrial laser scanning also has its shortcomings. First – especially in the field of engineering survey – the limited accuracy has to be considered. Although the instrument's verified accuracy is ± 5 mm, the terrestrial laser scanning is a capable additional technology besides the conventional engineering geodetic methods. Instead of measuring predefined, dedicated points, the entire visible structure can be captured that enable various investigations in the post-processing (e.g. cable movements, pylon deformation, etc.)

ACKNOWLEDGEMENT

Authors would like to thank to Burken Ltd. for providing the scanner for the investigations.

This paper was supported by the János Bolyai Research Scholarship of the Hungarian Academy of Sciences.

REFERENCES

Berényi, A., Lovas, T., 2009. Laser Scanning in Deformation Measurements. *GIM International*, 23(3), pp. 17-21.

Berényi, A., Lovas, T., Barsi, Á., Dunai, L., 2009. Potential of Terrestrial Laserscanning in Load Test Measurements of Bridges. *Periodica Polytechnica*, 53(1), pp. 25-33.

Lovas, T., Barsi, Á., Detrekői, Á., Dunai, L., Csák, Z., Polgár, A., Berényi, A., Kibédy, Z., Szöcs, K., 2008. Terrestrial Laserscanning in Deformation Measurements of Structures. In: *International Archives of Photogrammetry and Remote Sensing*, Vol. XXXVII, Part B5, pp. 527-531.

Lovas, T., Barsi, Á., Polgár, A., Kibédy, Z., Berényi, A., Detrekői, Á., Dunai, L., 2008, Potential of Terrestrial Laserscanning Deformation Measurement of Structures, Proc. ASPRS Annual Conference, Portland, USA, April 28 – May 2, p. 10.

Kersten, T., Mechelke, K., Lindstaedt, M., Sternberg, H., 2008, Geometric Accuracy Investigations of the Latest Terrestrial Laser Scanning, FIG Working Week 2008, Integrating Generations, Stockholm, Sweden, June 14-19, p. 16.

http://www.riegl.com/uploads/tx_pxpriegldownloads/10_DataSheet_Z420i_09-12-2009.pdf (accessed 15 Mar. 2010)